Phase-Regenerative Wavelength Conversion for BPSK and DPSK Signals

Kevin A. Croussore and Guifang Li

***Abstract*—Phase-regenerative wavelength conversion is demonstrated experimentally. The simultaneous combination of two nonlinear optical processes, phase conjugation and frequency conversion (Bragg scattering), produces phase-sensitive gain at two new idler wavelengths in addition to the original signal wavelength. This single-stage approach does not require phase-locking of the tunable pump. At maximum pump depletion, amplitude and phase regeneration occur simultaneously.**

***Index Terms*—All-optical regeneration, four-wave mixing (FWM), phase-sensitive amplification, wavelength conversion.**

I. Introduction

PHASE-SENSITIVE amplifiers (PSAs) offer several potential benefits compared to phase-insensitive amplifiers. Among these are the ability to compensate fiber chromatic dispersion [1], reduction of noise [2], the suppression of modulation instability [3] and reduction of noise-induced frequency [4], and phase [5] fluctuations. PSAs have attracted considerable attention for their prospective role in processing of optical signals. They are particularly appropriate for the amplification and regeneration of binary and differential phase-shift keyed signals (BPSK and DPSK). Several recent publications have highlighted the capabilities of different PSA implementations in this role [6]–[11]. To this point, PSAs based on both nonlinear optical loop mirrors and degenerate four-wave mixing (FWM) in fiber have been implemented experimentally for DPSK or BPSK regeneration [6], [7], [9]. In these schemes, the input and output signal frequencies are identical.

A recent paper outlined the FWM processes that produce PSA directly in fiber [10]. The two-stage process [Bragg scattering (BS), followed by phase conjugation (PC)] in [10] can also produce PSA at a new idler wavelength, in principle providing phase-regenerative wavelength conversion (PR-WC) of the signal. A limited analysis of this capability was provided in a later publication [12]. In this letter a similar, but distinct, process is studied, in which PSA occurs at two new wavelengths during a single stage of nonlinear interaction. For reference, it is referred to as simultaneous BS-PC. The frequency arrangement and constituent nonlinear interactions for this process are shown in Fig. 1. In the scalar case considered in experiments, all waves share the same polarization (*scalar* simultaneous BS-PC). The signal frequency satisfies the relationship $\omega_2 = (\omega_1 + \omega_3)/2$ where Waves 1 and 3 are the usual pumps for PSA [10]. Pump 5 is the WC pump, and Waves 4 and 6 are the wavelength-converted, phase-regenerated idlers. The frequency of the WC pump is tunable, and the idler frequencies are given by $\omega_{4,6} = \omega_5 \mp (\omega_1 - \omega_3)/2$.

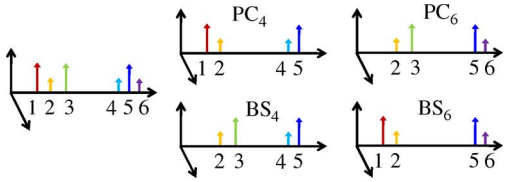

Fig. 1. Frequency allocation (left) and constituent nonlinear interactions for Waves 4 (center) and 6 (right).

The implementation discussed here resolves two notable challenges to the two-stage scheme [10], in addition to its inherent reduction of complexity and use of nonlinear materials. First, in the two-stage scheme all pumps, including the WC pump, must be phase-locked to the input signal [10]. Considering the WC pump should be tunable, this can be difficult to satisfy. Second is the required optimization of energy exchange between signal and idler in the first stage, which determines whether or not the second stage provides phase regeneration. The single-stage scheme eliminates the need for such optimization and experiments show it also provides stronger phase-sensitive gain (PSG) than other PSA implementations. One distinguishing feature of the single-stage scheme is that the idlers are initially produced with perfectly binary phases [13], negating the requirement for large conversion efficiency. As with all PSAs, phase regeneration is achieved at the expense of added amplitude noise (AN); however, this AN reduces as the conversion efficiency increases.

II. Experimental Setup

The experimental setup is shown in Fig. 2. The arrangement is identical to that used in a previous PSA experiment [6] with the following exceptions. An additional tunable laser serving as the WC pump is coupled in through the 10% output of a 90/10 coupler and amplified with the other waves. The power of this pump was adjusted to be equal to that of each PSA pump. Additional polarization control was required to launch parallel linear polarizations of all four waves. The Bi-HNLF has length, effective

Manuscript received July 31, 2008; revised September 29, 2008. Current version published January 08, 2009. This work was supported in part by Defense Advanced Research Projects Agency (DARPA) under Contract DAAD1702C0097 and by the National Science Foundation under Grant DGE 014418.

K. A. Croussore is with Fujitsu Laboratories of America, Fujitsu Network Communications, Richardson, TX 75082 USA (e-mail: kcrousso@creol.ucf.edu; kevin.croussore@us.fujitsu.com).

G. Li is with the University of Central Florida, College of Optics and Photonics, Orlando, FL 32816 USA (e-mail: gli@creol.ucf.edu).

Color versions of one or more of the figures in this letter are available online at http://ieeexplore.ieee.org.

Digital Object Identifier 10.1109/LPT.2008.2008313

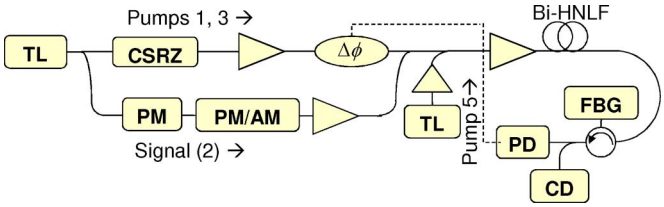

Fig. 2. Experiment setup. TL: tunable laser. PM/AM: phase/amplitude modulation. PD: photodiode (100-MHz bandwidth.) For further details see [6].

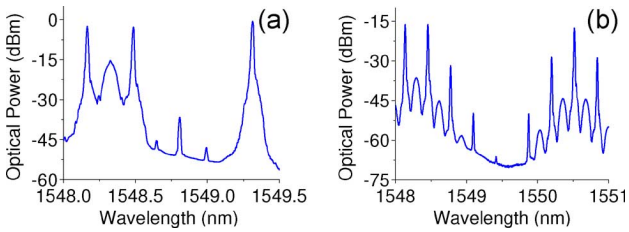

Fig. 3. (a) Typical PR-WC input spectrum after booster amplifier. The WC pump is near 1549.3 nm. (b) PR-WC output for small pumping power.

nonlinearity, dispersion, total splicing loss, and distributed loss of 5.64 m, 1100/W/km, −290 ps/nm/km, 3.1 dB, and 1.4 dB/m, respectively. One output idler was selected using a fiber Bragg grating (FBG) with ∼18-GHz bandwidth (full-width at half-maximum). The power of this idler was monitored in order to stabilize the input phases of the two PSA pumps relative to the signal average phase. No phase stabilization of the WC pump was performed. We note the idler power must be monitored for proper phase stabilization, since the phase-dependencies of the signal and idler gains differ. For all experiments reported here, the signal was 10-Gb/s nonreturn-to-zero BPSK with pseudo-random binary sequence length $2^{15} - 1$. Distortion is added to this signal using additional phase and amplitude modulation at frequencies ranging from 4–6 GHz. The amplitudes of the distortions are apparent in the results that follow. The feedback circuit compensates slow phase drifts (kilohertz or megahertz) resulting from vibrations or thermal drift, but not phase changes due to data modulation or noise emulation. The FBG output is divided for feedback and coherent detection (CD) using an independent local oscillator (LO) tuned near the idler wavelength as in [9]. The lasers for signal, PSA and WC pumps and LO all have kilohertz linewidths. CD is enabled by digital signal processing software (EnvCalc, commercially available) that tracks the relative LO/idler phase and calculates the idler electric field. This also allows differential demodulation in the software domain.

III. Results

Fig. 3 shows optical spectra at the input of the wavelength converter and at the output under small pumping power. The frequency arrangement differs slightly from that of Fig. 1 due to the filters available for experiments (a tunable filter located near the WC pump is required). The signal is located at 1548.3 nm (PSA pumps are spaced symmetrically 20 GHz on either side). Fig. 3(b) clearly shows two primary phase-modulated idlers

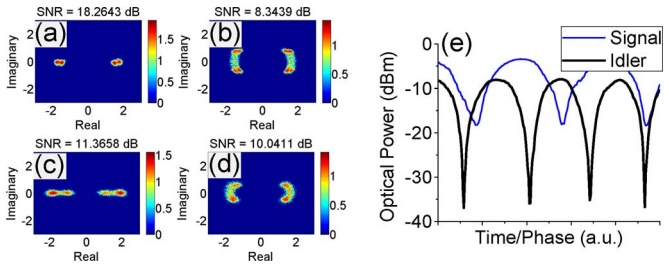

Fig. 4. Constellations for back-to-back signal (a) noiseless and (b) with phase distortions added; (c) Idler 4 after regenerative wavelength conversion; (d) signal output. (e) Measurement of the signal and idler power against changing signal input phase (uncorrelated time axes for individual measurements).

generated symmetrically about the WC pump, which was located near 1550.5 nm. In experiments, the shorter-wavelength idler was of slightly better quality and was used for measurements. Additional pump–pump FWM products as well as new idlers generated through cascaded FWM are visible.

A distinguishing feature of simultaneous BS-PC is that the idlers are phase-regenerated at initial generation. This was verified by measurement of the idler electric field with minimal pumping power. Fig. 4 shows the constellations for four cases: back-to-back (B2B) signal without and with phase noise (PN) [(a) and (b), respectively], the idler measured with only 100-mW total pumping power (c), and the corresponding output signal (d). The received idler power was about −18 dBm, and the constellations represent measurement of about 15 000 consecutive bits. The PN of the signal converts to AN at the idler wavelength; however, the idler PN is roughly equivalent to that of the B2B, noiseless signal. In contrast, the signal output shows no reduction of PN. Residual PN at the idler wavelength arises from broadband amplified spontaneous emission (ASE) after the booster amplifier, which cannot be removed in this experiment. For the B2B noiseless case, the anomalous distribution results from the combination of polarization modulation of the signal occurring at the transmitter and CD. Fig. 4(e) compares the measured PSG ($\mathrm{PSG} = 10 \cdot \log(P(\phi_{\max})/P(\phi_{\min}))$ for the signal and idler at a pumping power around 300 mW (about 100 mW for each pump). The signal phase was varied at a slow kilohertz rate by scanning a free-space delay line with data modulation turned OFF. While the signal PSG is roughly 15 dB, the idler achieves a PSG exceeding 30 dB even though the maximum idler power is 5 dB less than that of the signal. Large PSG of the idler is due to strong quadrature attenuation, rather than in-phase amplification, which is maximized when the idler is produced by BS and PC equally.

The WC efficiency for the results of Fig. 4 is small ($\sim$ −15 dB), and even though the phase characteristics of the idlers are excellent, a large amount of AN is generated due to PN → AN conversion. In realistic systems, such AN will not be tolerable and should be removed, possibly through use of another process. PSAs may also act as limiting amplifiers [7]–[9], reducing noise through saturation of FWM gain; this applies in PR-WC as demonstrated below. To generalize the previous results, a signal suffering both AN and PN was launched together with the three pumps, and the output idler electric field

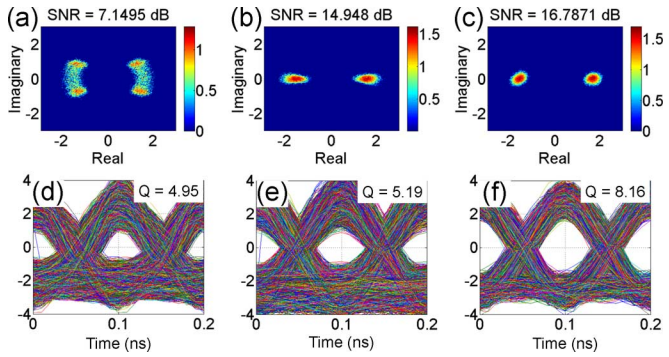

Fig. 5. (a)–(c) Constellations and eye diagrams for (d)–(f) differential detection for input signal [(a), (d)], output idler with best phase statistics [(b), (e)] and for maximum conversion [(c), (f)]. A 2-nm wavelength shift.

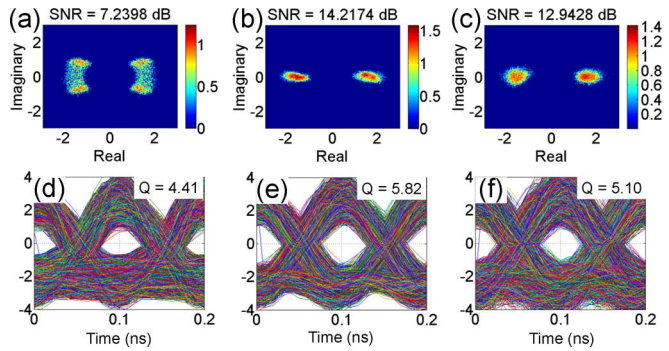

Fig. 6. Constellations and eye diagrams for 5-nm wavelength shift.

was characterized while the pumping power was increased. Initially the WC pump was tuned to provide a 2-nm wavelength shift of the idler from the input signal. At each launch power, the differential phase Q-factor (DPQ) and signal-to-noise ratio (SNR) were calculated from the idler constellation. Fig. 5 summarizes the results, giving constellations for the B2B signal, the idler with minimized PN, and the idler at highest conversion efficiency, which also produces a minimum of AN and the best SNR. The minimum standard deviation of differential phase was 6.25°. This increased at maximum conversion efficiency to around 8.4° due to a combination of idler self-phase modulation (small), pump and signal cross-phase modulation, and additional ASE produced at higher launch powers. This degraded the DPQ by about 1.23 dB, however, the SNR reached a maximum of 16.9 dB. This was an improvement of about 10 dB, indicating a substantial overall reduction of noise. At the highest launch power the idler conversion efficiency reached a value near $+1$ dB. Fig. 5 also shows eye diagrams that were calculated for *differential detection*, performed in the software domain after measurement of the electric field. These reveal a significant increase of the eye opening and improvement of the eye Q-factor as well.

The practical range for WC is determined mainly by the dispersive characteristics of the fiber. For fully regenerative WC, depletion of the pumps is crucial for reducing AN, which implies phase-matching must be maintained. However, phase-regenerative WC can be obtained over almost any range, regardless of conversion efficiency. In experiments, the availability of tunable filters limited the WC range to 5 nm. Results obtained for this wavelength shift are given in Fig. 6. Compared to the previous case, the results were somewhat degraded. For example, the SNR at minimal PN dropped by ∼0.5 dB, and the SNR at maximum conversion efficiency dropped by about 4 dB. This reduction was determined to result from two factors not related to the fundamental performance of PR-WC. First, the noise on the input signal for the 5-nm case was slightly larger. Second, the aforementioned problem of signal polarization modulation [Fig. 4(a)] caused excess noise for the latter case. Overall, the conversion efficiencies and measured PSG for the two wavelength shifts were similar, implying phase-matching did not significantly change the results. This argument is supported by theory, given that the pump–signal and pump–idler frequency spacing is only ∼20 GHz.

IV. Conclusion

This letter demonstrates the first convincing method for PR-WC based on PSA. Unlike standard implementations of PSA, phase-regeneration occurs at the new idler wavelengths at initial generation and is preserved up to idler gain saturation. The added capability of wavelength conversion comes with only a small increase in complexity compared to existing PSAs, thus serving to make those devices more practical through increased flexibility.

References

[1] R. Li, P. Kumar, and W. L. Kath, "Dispersion compensation with phase-sensitive optical amplifiers," *J. Lightw. Technol.*, vol. 12, no. 3, pp. 541–549, Mar. 1994.

[2] R. Loudon, "Theory of noise accumulation in linear optical-amplifier chains," *IEEE J. Quantum Electron.*, vol. 21, no. 7, pp. 766–773, Jul. 1985.

[3] W. Imajuku and A. Takada, "Reduction of fiber-nonlinearity-enhanced amplifier noise by means of phase-sensitive amplifiers," *Opt. Lett.*, vol. 22, no. 1, pp. 31–33, 1997.

[4] H. P. Yuen, "Reduction of quantum fluctuation and suppression of the Gordon-Haus effect with phase-sensitive linear amplifiers," *Opt. Lett.*, vol. 17, no. 1, p. 73, 1992.

[5] Y. Mu and C. M. Savage, "Parametric amplifiers in phase-noise-limited optical communications," *J. Opt. Soc. Amer. B*, vol. 9, no. 1, p. 65, 1992.

[6] K. Croussore and G. Li, "Phase regeneration of NRZ-DPSK signals based on symmetric-pump phase-sensitive amplification," *IEEE Photon. Technol. Lett.*, vol. 19, no. 11, pp. 864–866, Jun. 1, 2007.

[7] K. Croussore *et al.*, "Phase-and-amplitude regeneration of differential phase-shift keyed signals using a phase-sensitive amplifier," *Opt. Express*, vol. 14, no. 6, pp. 2085–2094, 2006.

[8] A. Bogris and D. Syvridis, "RZ-DPSK signal regeneration based on dual-pump phase-sensitive amplification in fibers," *IEEE Photon. Technol. Lett.*, vol. 18, no. 20, pp. 2144–2146, Oct. 15, 2006.

[9] K. Croussore and G. Li, "Phase and amplitude regeneration of differential phase-shift keyed signals using phase-sensitive amplification," *IEEE J. Sel. Topics Quantum Electron.*, vol. 14, no. 3, pp. 648–658, Mar. 2008.

[10] C. J. McKinstrie and S. Radic, "Phase-sensitive amplification in a fiber," *Opt. Express*, vol. 20, pp. 4973–4979, 2004.

[11] M. E. Marhic, C. H. Hsia, and J. M. Jeong, "Optical amplification in a nonlinear fiber interferometer," *Electron. Lett.*, vol. 27, pp. 210–211, 1991.

[12] C. J. McKinstrie *et al.*, "Quantum mechanics of phase-sensitive amplification in a fiber," *Opt. Commun.*, vol. 257, no. 1, pp. 146–163, 2006.

[13] K. Croussore and G. Li, "Phase-regenerative DPSK wavelength conversion," in *IEEE 20th Annual Meeting LEOS*, Orlando, FL, 2007.